Penetration Process of a Hydrated Deep Eutectic Solvent Through the Stratum Corneum and its Application as a Protein Penetration Enhancer

Mina Sakuragi,* Emika Maeda, and Katsuki Kusakabe[a]

The penetration mechanism of choline chloride-glycerol deep eutectic solvent (DES) through the stratum corneum (SC) as a potential solvent for a novel enhancer of protein penetration into the skin was investigated in a wide and small angle X-ray diffraction study. We found that DES penetrated through intercellular lipids but not the corneocytes. DES seemed to extract a portion of lipids of the short lamellae in the SC. Hydrated DES with a DES to water weight ratio of 9 to 1 (9DES-1H_2O) showed the strongest interaction with the lipids in the SC compared with water, DES, and hydrated DESs with another weight ratio of DES to water (DES:water = 8:2). In a skin penetration test with a fluorescently labelled lysozyme, 9DES-1H_2O increased the amount of penetration through the SC by two-fold compared with HEPES buffer.

1. Introduction

The stratum corneum (SC), which is located in the outermost layer of the skin, plays an important role in barrier function. Accordingly, the performance of transdermal drug delivery systems are affected by the characteristics of SC.[1,2] The SC is composed of corneocytes and intercellular lipid lamellae. In general, hydrophobic molecules with low molecular weight mainly penetrate the intracellular lipid layer pathway in the SC[3] and exhibit high transdermal permeability.[4,5] The lipid layer forms mainly two types of lamellar structures, short lamellar (S–La) and long lamellar (L–La) structures that have repeat distances of 6 nm and 13.5 nm, respectively, in both mouse and human SC.[1,6–8] Ohta et al. investigated changes in the lipid lamellar structures of hairless mouse at various water contents by small-angle X-ray diffraction (SAXD),[9] suggesting that S–La included the water phase but not L–La. Wide-angle X-ray diffraction (WAXD) shows the peaks of two types of hydrocarbon packing structures at the lateral organization level of the lipid lamellae:[10,11] a hexagonal chain packing (Hex) structure with 0.41 nm lattice spacing and an orthorhombic-chain packing (OR) structure with lattice spacings of 0.37 nm and 0.41 nm. The temperature dependence of peak intensities in the simultaneous SAXD and WAXD analyses revealed that the hydrocarbon chains of L–La and S–La were organized into the Hex and OR phases, respectively.[10]

Biologic medical products, such as proteins, polysaccharides, vaccines, and nucleic acids, are rapidly developing these days.[12] However, these products rarely penetrate the SC layer due to hydrophilic macromolecules and require a penetration enhancer, such as physical (e.g. microneedle, iontophoresis, and electroporation[13]) or chemical enhancers, to penetrate the skin, especially the SC layer. Regarding chemical penetration enhancers, various types of products have been investigated,[14] and further development of biomaclomolecules that act as skin penetration enhancers and elucidation of their penetration mechanism are urgently needed.

Ionic liquids (ILs) are organic salts composed of relatively large asymmetric organic cations and inorganic anions. ILs can be used as potential solvents to improve the solubility of various molecules.[15–17] Recently, IL has been reported as a potential vehicle for transdermal delivery. Zakrewsky et al.[18] evaluated a number of ILs for the enhancement of antibiotic delivery across the skin. As a result, choline-geranate IL (CAGE) enhanced the skin penetration for the drug without skin irritation. For the efficacy of CAGE in the skin permeation of biomacromolecules, CAGE can deliver proteins such as insulin,[19] bovine serum albumin, and ovalbumin.[20] Wu et al. reported enhanced transdermal permeation of polysaccharides using choline-maleic acid-based ILs.[21] The improvement in the amount of permeation is probably due to the extraction of lipids by ILs. However, the penetration process of ILs across the SC is still unknown.

Deep eutectic solvents (DESs), which are composed of a hydrogen bond acceptor such as a quaternary ammonium salt, choline chloride and hydrogen bond donor such as urea or glycerol, have physical properties similar to ILs,[22–24] so DESs were classified as IL analogues.[25,26] For choline chloride-glycerol DES, each component forms interwoven network via the interaction of O_{cho}—H···Cl^-···H—O_{gly} (or O_{cho}···Cl^-···O_{gly}).[27] Recently, DESs have attracted attention as an alternative to ILs due to

[a] Dr. M. Sakuragi, E. Maeda, Prof. K. Kusakabe
Faculty of Engineering
Department of Nanoscience
Sojo University
4-22-1 Ikeda, Nishi-ku, Kumamoto City 860-0082 (Japan)
E-mail: d08b0101@nano.sojo-u.ac.jp

Supporting information for this article is available on the WWW under https://doi.org/10.1002/open.202000114

some potential advantages, such as low cost, nontoxicity, and high biodegradability.[28,29] DESs also exhibit potential as solvents for enhancing the solubility of some molecules as well as ILs.[30–32] A therapeutic deep eutectic system (TDES) with an active pharmaceutical ingredient (API) as one of its components has also been developed in recent years.[33,34] TDES can increase the solubility, permeation, and adsorption of API. Generated by diluting DESs with water, hydrated DESs have also attracted attention.[35] Adding water to DESs can significantly reduce the viscosity of DESs and improve long solvent-transfer times and slow molecular diffusion.[36,37]

In this paper, DES was prepared from a mixture of choline chloride and glycerol. Then, water was added to the mixture, and the hydrated DESs were used in this study. The penetration mechanism of DES, hydrated DES, and water into the SC were evaluated using SAXD and WAXD. Furthermore, the skin penetration of the model protein lysozyme dissolved in hydrated DES was investigated in comparison with water.

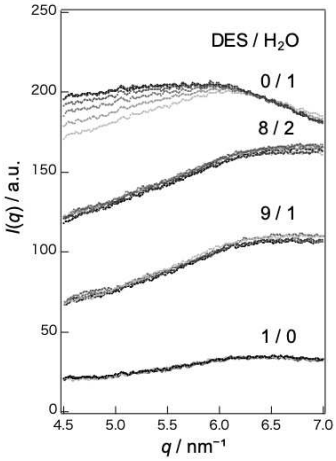

Figure 1. Change in the broad peak at 1 nm due to the soft keratin in the corneocytes when applying each solvent. The colors of the profiles change from gray to black over time.

2. Results and Discussion

2.1. Solvents Penetration into Corneocytes

We compared the interaction mechanism across the SC among DES, hydrated DES, and water. Each hydrated DES with varying water content was named according to the weight ratio of DES to H_2O. For example, the hydrated DES at DES/H_2O = 9/1 was 9DES-1H_2O. Hydrated DES reduced the viscosity compared to an anhydrous DES at room temperature (DES; 270 mPa s, 9DES-1H_2O; 32.0 mPa s, 8DES-2H_2O; 9.7 m Pa·s, 7DES-3H_2O; 5.8 mPa s, 5DES-5H_2O; 1.39 mPa s). Reducing the viscosity increases solvent transfer and molecular diffusion. Dai et al.[38] reported that the physical properties of DESs such as solubilizing capacity could be altered by varying water content. Using UV-Vis spectroscopy, we found that the saturated solubilities of lysozyme in DES or hydrated DES (DES/water = 9/1, 8/2, and 7/3) were 5.2, 22.7, 72.2, and 48.9 mg/mL, respectively. We expected that a hydrated DES at around the DES/water ratio of 8/2 may also exhibit a high affinity for the SC components as is the case with the solubility of lysozyme. We also focused on 9DES-1H_2O because Weng et al.[27] showed that the direct hydrogen-bonding between choline and glycerol for choline chloride-glycerol DES containing 10.1 wt% water became stronger than the anhydrous DES, and further water addition weakened the interaction between DES components. Therefore, we selected 9DES-1H_2O and 8DES-2H_2O for hydrated DES.

SC is composed of corneocytes and lipids. The penetration of water, DES, and hydrated DES through corneocytes containing soft keratin was investigated. Of note, the SC tested here exhibits very diffuse structural peaks with lattice spacings of 0.46 nm and 1.0 nm derived from soft keratin.[6] In our case, the peak at 0.46 nm was not detected clearly, but the broad peak around 1 nm (q = 6.3 nm^{-1}) was observed (Figure 1). When the SC was exposed to water, the shape of the broad peak changed over time due to the swelling of water in soft keratin. When the SC was exposed to solvents containing DES, approximately no change in shape was noted. These results indicated that water penetrates the corneocytes, whereas DES and hydrated DES did not. Bouwstra et al. also reported the uptake of water into corneocytes but not in the intercellular regions based on FT-IR and cryo-scanning electron microscopy.[39]

2.2. Transition of the Lamella Structure in SC

Figure 2 shows the SAXD profile of the SC in the q range from 0.5 to 3.0 nm^{-1}. When the SC was exposed to water, the diffraction profiles of SC exhibited several peaks from L–La as shown by the arrows in Figure 2a. When water was applied to the SC, the intensities of these peaks increased with time. Charalambopoulou et al.[40] reported that the neutron scattering intensity of the SC increased with increasing water contents in the SC in a very small angle region. The present result supports their results. In addition, the clear second peak of L–La did not seem to change the area and the position. Hatta et al.[41] demonstrated that the spacing of L–La was unchanged, while the S–La spacing increased from 5.8 to 6.6 nm as the water content of the SC increased from 12 to 50 wt%. They also showed that the first peak of S–La was not observed clearly when the water content of the SC was 0 wt% and greater than 50 wt%. In this study, we could not observe the clear S–La peak with a lattice spacing of 6 nm (q = 1.05 nm^{-1}). Accordingly, water was absorbed immediately after exposure to the SC, and the water content might be greater than 50 wt%. Regarding exposure to DES (Figure 2b), the peak intensity at q = 0.92 nm^{-1} decreased over time, while the high-order Bragg peaks of L–La were almost unchanged. Since the first-order broad peak of S–La at q = 1.05 nm^{-1} overlaps with the second peak of L–La at q = 0.92 nm^{-1}, this change may be due to a decrease in the S–La peak. When hydrated DES was applied to the SC, the behavior of the profiles was similar to the DES results (Figure 2c and d). DES and hydrated DES appear to extract a portion of lipids from S–La, partly disrupting the S–La structure. It has

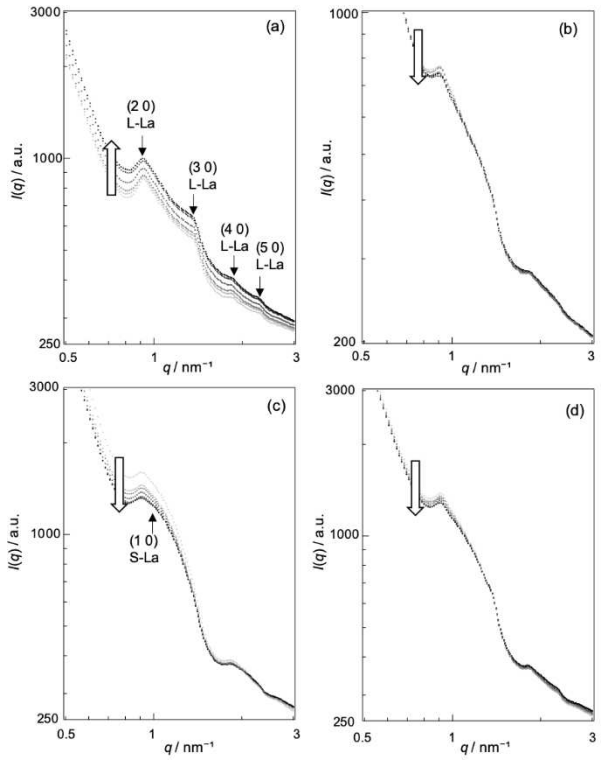

Figure 2. Change in SAXD profiles over time (5, 10, 15, 30, 50 and 60 min) from gray to black after applying (a) H_2O, (b) DES, (c) 9DES-1H_2O, and (d) 8DES-2H_2O.

been shown that CAGE, composed of choline and geranate, was able to extract lipids in the SC with FT-IR spectra.[19,20] Figure S1 shows FT-IR spectra of the SC before and 24 h after application of each sample in the lipid region. Results showed that DES and hydrated DES extracted lipids in the SC by FT-IR as is the case with CAGE (Figure S1), while water did not extract them at all. The result is consistent with the SAXS results. We also found that the intensity of 9DES-1H_2O changed significantly compared to that of DES and 8DES-2H_2O. It has been reported that DES and hydrated DES caused the aggregation of surfactants due to the solvophobic interaction between DES and the hydrocarbon chains of surfactants.[30,31] Since the strength of the direct hydrogen-bonding interaction between choline and glycerol becomes maximum at DES containing 10.1 wt% water,[27] the solvophobic interaction between 9DES-1H_2O and hydrocarbon chains of lipids in the SC seems to be the strongest among these solvents. As a result, 9DES-1H_2O could interact with the lipids in the SC most strongly and disrupt the S–La structure the most.

2.3. Transition of Hydrocarbon Packing Structure of the Lipid Layer in SC

In WAXD studies, we observed two diffraction peaks at lattice spacings of 0.41 and 0.37 nm. The lattice spacing of 0.41 nm is derived from the Hex and OR structures for the lateral packing of hydrocarbons in the lipid lamellar structure. The lattice spacing of 0.37 nm is exclusively derived from the OR structure. Figure 3a and 3b shows the normalized peak area of the peaks at 0.41 and 0.37 nm at 60 min after feeding each solvent, respectively. The results showed that 9DES-1H_2O significantly disturbed the lipid packing structures compared to other solvents. The statistical evaluation of these normalized peak areas 60 min after application of the samples to the SC was also performed (Figure S2). The data exhibited good reproducibility. To discuss whether these solvents affect Hex or OR, the apparent abundance ratio $R_{H/O}$ was defined as follows:[42,43]

$$R_{H/O} = \frac{I_{0.41}}{I_{0.37}} = \frac{I^O_{0.41} + I^O_{0.37}}{I^O_{0.37}} = \frac{I^O_{0.41}}{I^O_{0.37}} + \frac{I^H_{0.41}}{I^O_{0.37}}$$

where I represents the peak area, the subscripts of 0.41 and 0.37 represent the lattice spacings of each peak, and superscripts O and H indicate OR and Hex, respectively. The first term is constant, while the second term indicates the ratio of Hex to

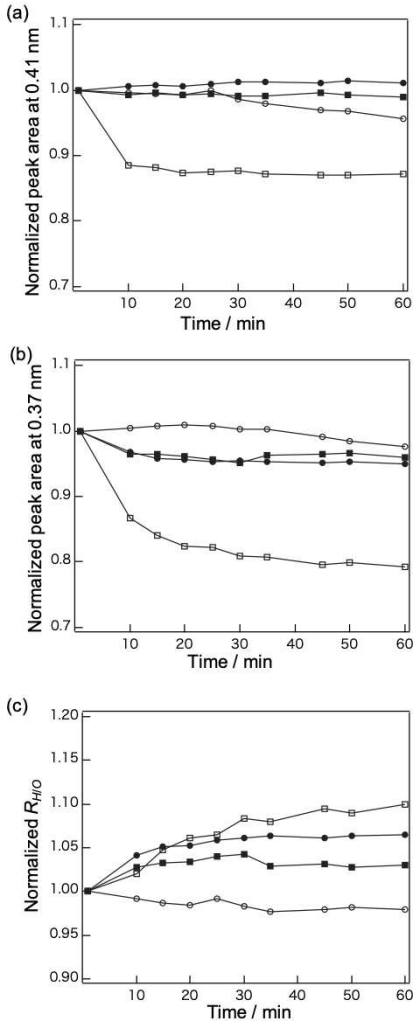

Figure 3. Time course of the normalized peak area at 0.41 nm (a) and 0.37 nm (b) when exposing each sample, and the time course of the normalized intensity ratio (c). Open circle, closed circle, open square, and closed square represent water, DES, 9DES-1H_2O, and 8DES-2H_2O, respectively.

OR. In this study, DES and hydrated DES increased $R_{H/O}$ with time (Figure 3c). This finding indicates that the Hex structure is dominant in the lipid packing. This fact indicates that these solvents tend to disturb OR rather than Hex. Additionally, 9DES-1H_2O disrupted the OR to the greatest extend among these solvents. This result is consistent with the SAXD result that 9DES-1H_2O significantly disrupted S–La compared to other solvents because the hydrocarbon chains of L–La and S–La were organized into Hex and OR, respectively.

2.4. Skin Penetration

For skin penetration studies, we used FITC-labelled lysozyme as a model protein and compared the level of skin penetration of the lysozyme in 9DES-1H_2O with that in HEPES buffer. X-ray diffraction studies indicated that 9DES-1H_2O showed the strongest interaction with the lipids in S–La among the prepared solvents as mentioned above. Thus, 9DES-1H_2O is expected to be useful as a skin penetration enhancer for proteins.

DES composed of glycerol and choline chloride can dissolve lysozyme without unfolding at 20 °C.[44] In this study, we confirmed that the three-dimensional structure of lysozyme in DES was almost unchanged compared to that in water using SAXS (Figure S3). A transdermal penetration test was performed using FITC-lysozyme dissolved in 9DES-1H_2O or HEPES buffer and full-thickness skin with subcutaneous fat removed. Although we tried to determine the concentration of FITC-lysozyme after skin penetration using fluorescence spectroscopy, the reproducibility of the data was low due to the dilute concentrations. Therefore, we compared the fluorescent microscopic images of the skins used in skin penetration tests of FITC-lysozyme in 9DES-1H_2O and HEPES buffer as shown in Figure 4a and b. The fluorescent brightness at the SC emitted from FITC-lysozyme in 9-DES-1H_2O was considerably increased compared with that in HEPES buffer. This finding indicates that 9-DES-1H_2O can enhance the permeation of FITC-lysozyme into the SC compared to HEPES buffer. Subsequently, the level of FITC-lysozyme penetration through the SC was determined based on skin penetration tests. As shown in Figure 4c, hydrated DES facilitates an approximately two-fold increase in lysozyme penetration through the SC compared with HEPES buffer. Statistical analysis revealed a significant difference between 9DES-1H_2O and HEPES buffer ($p = 0.0248$).

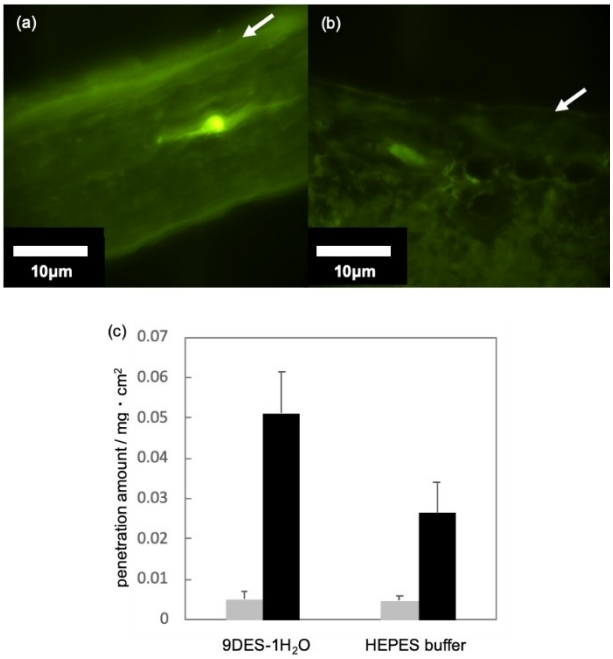

Figure 4. Fluorescence microscope images of FITC-Lys into hairless mouse skin treated with 9DES-1H_2O (a) and HEPES buffer (b) for 48 h. The arrows indicate the position of the SC. The amount of FITC-lysozyme penetration through the SC after 3 h (gray) and 24 h (black) (c). Each value represents the mean ± S.D. (n = 3). *$p < 0.05$ vs HEPES buffer.

3. Conclusions

In this study, we examined the potential of hydrated DES to enhance the skin permeation of lysozyme and the penetration mechanism of hydrated DES into the SC. SAXD and WAXD results suggest that water can penetrate corneocytes in SC, whereas DES and hydrated DES cannot. The results also showed that DES and hydrated DES extract a portion of lipids in S–La, partly disrupt the S–La structures, and disrupt the OR hydrocarbon packing structure in S–La. In addition, we found that 9DES-1H_2O exhibited the strongest interaction with lipids in S–La among the prepared solvents probably due to the strongest solvophobic interaction between 9DES-1H_2O and the hydrocarbon chains of the lipids in S–La. In the skin penetration study, 9DES-1H_2O increased the penetration of lysozyme through the SC compared to HEPES buffer due to the disruption of S–La through partial extraction of lipids. Although hydrated DES does not facilitate deep lysozyme penetration into the skin, it represents a potential solvent that acts as a novel enhancer of transcutaneous immunization targeting antigen-presenting cells abundant in dermis and epidermis.

Experimental Section

Materials

Glycerol and chicken egg lysozyme (a basic protein, molecular weight: 14.3 kDa, electric point: 11.35) were purchased from FUJIFILM Wako Pure Chemicals. The shape of lysozyme is close to an ellipsoid, and its size in water is reported to be a rotational axis of 3.5 nm and equatorial radii of 1.45 nm by SAXS analysis.[45] Choline chloride was purchased from Sigma Aldrich. The skins of seven-week-old male hairless mice from which subcutaneous fat was removed were purchased from Japan SLC, Inc. Fluorescein 5′-isothiocyanate (FITC) was purchased from Dojindo Lab. Trypsin and trypsin inhibitor were purchased from Fujifilm Wako Pure Chemical Corporation (Japan).

DES Preparation

The reagent choline chloride was vacuum dried for more than 2 days at room temperature. DES was prepared by mixing choline chloride and glycerol at a 1:2 molar ratio at 80 °C and stored at 40 °C in an oven as reported previously.[31] Then, 10 and 20 wt% water was added to the mixture, and the hydrated DESs were used in this study.

Sample Preparation for X-Ray Diffraction Measurements

The skin of seven week-old male hairless mouse was immersed in 0.1 % trypsin in 10 mM phosphate buffer, pH 7.4, at 4 °C overnight, and the SC was separated from the skin after incubation for 4 h at 37 °C. The SC was immersed in 0.1 % trypsin inhibitor, washed with water, and dried in a vacuum chamber overnight.[43]

Characterization

SAXD and WAXD measurements were performed at the beamline 40B2 at SPring-8, a synchrotron radiation facility in Japan. The X-ray diffraction profiles were recorded using a Pilatus detector. The wavelength was 0.1 nm, and the sample-to-detector distance was approximately 400 mm. A piece of the sample of the dried SC was placed inside a small steel washer between two Kapton sheets. A sample measurement was taken at room temperature for 15 s.

Lysozyme Labelling

FITC-labelled chicken egg lysozyme (FITC-lysozyme) was prepared according to the reference.[46] FITC and lysozyme were dissolved in 100 mM borate buffer at pH 9.1 to yield 110 μM protein and label. After incubation for 90 min at room temperature, FITC-lysozyme solution was dialyzed using cellulose dialysis tube with 3500 molecular weight cut off in HEPES buffer solution (20 mM HEPES, 0.1 mM EDTA at pH 7.4) in a refrigerator at 4 °C. The concentration of FITC and lysozyme in the solution was measured using a UV spectrophotometer (SIMADZU UV-1800) based on the extinction coefficients of 73,000 $M^{-1}cm^{-1}$ at 494 nm and 45,200 $M^{-1}cm^{-1}$ at 280 nm for FITC and 37,800 $M^{-1}cm^{-1}$ at 280 nm for lysozyme. The molar ratio of FITC to lysozyme was 0.52.

Skin Penetration Experiments

The SC obtained by the above method was immersed in water for 40 min, and then the SC was dehydrated under airflow until the water content in the SC reached 30 wt%. The water content of the SC was estimated from the weight difference before and after hydration. The skin penetration test was performed using Franz diffusion cells (PermeGear, Inc., USA) with a diameter of 5.0 mm. Then, 10 mM phosphate buffer solution was placed in the receptor chamber, maintained at 37 °C and continuously stirred at 600 rpm. Full-thickness skin with subcutaneous fat removed or the SC containing 30 wt% water was placed on the receptor chamber. Then, 50 μL of the FITC-lysozyme solution in HEPES buffer or in 9DES-1H_2O (1 mg/mL lysozyme concentration) was placed on the SC surface. After 24 or 48 h, the FITC-lysozyme concentration in the receptor chamber was determined using a fluorescence spectrometer (PerkinElmer, LS-55). Fluorescence measurements were performed at 25 °C with a 10 mm path-length quartz cell. FITC-lysozyme was excited at $\lambda_{ex} = 470$ nm; its emission was recorded at $\lambda_{em} = 520$ nm. After the skin penetration test, the full-thickness skin sample was wiped, washed with water, and immersed in 10 % formalin. Subsequently, the skin was vertically cut into 20-μm thick slices, and the tissue sections were mounted on microscope slides produced by Tokushima Molecular Pathology Institute, Inc. The tissue sections were observed with a fluorescence microscopy (Shimadzu group, RF-6000). Data are presented as the means ± S.D. (n = 3). Significant differences among solvents were determined using the one-tail unpaired student *t*-test. A probability value of $p < 0.05$ was considered to indicate a statistical significance.

Acknowledgements

Synchrotron radiation experiments were conducted at SPring-8 BL40XU (No. 2018A1367) and BL40B2 (No. 2019A1225). We thank Dr. Noboru Ohta and Dr. Hiroshi Sekiguchi for experimental help at SPring-8. The present work was supported by a Grant-in-Aid for Young Scientists from the Ministry of Education, Culture, Sports, Science and Technology of Japan (JP19K15367).

Conflict of Interest

The authors declare no conflict of interest.

Keywords: deep eutectic solvents · drug delivery · stratum corneum · lysozyme · X-ray diffraction

[1] E. H. Mojumdar, J. A. Bouwstra, *Cosmetic Formulation: Principles and Practice*, CRC Press **2019**, Chapter 3, *47-60*.
[2] D. S. Shaker, R. A. Ishak, A. Ghoneim, M. A. Elhuoni, *Sci. Pharm.* **2019**, *87*, 17.
[3] M.-A. Bolzinger, S. Briançon, J. Pelletier, Y. Chevalier, *Curr. Opin. Colloid Interface Sci.* **2012**, *17*, 156–165.
[4] S. Wiedersberg, R. H. Guy, *J. Controlled Release* **2014**, *190*, 150–156.
[5] I. B. Pathan, C. M. Setty, *Trop. J. Pharm. Res.* **2009**, *8*, 173–179.
[6] J. A. Bouwstra, G. S. Gooris, J. A. van der Spek, S. Lavrijsen, W. Bras, *Biochim. Biophys. Acta* **1994**, *1212*, 183–192.
[7] J. A. Bouwstra, G. S. Gooris, J. A. van der Spek, W. Bras, *J. Invest. Dermatol.* **1991**, *97*, 1005–1012.
[8] A. Nakaune-Iijima, A. Sugishima, G. Omura, H. Kitaoka, T. Tashiro, S. Kageyama, I. Hatta, *Chem. Phys. Lipids* **2018**, *215*, 56–62.
[9] N. Ohta, S. Ban, H. Tanaka, S. Nakata, I. Hatta, *Chem. Phys. Lipids* **2003**, *123*, 1–8.
[10] I. Hatta, N. Ohta, K. Inoue, N. Yagi, *Biochim. Biophys. Acta* **2006**, *1758*, 1830–1836.
[11] J. Bouwstra, G. Gooris, M. Salomons-de Vries, J. Van der Spek, W. Bras, *Int. J. Pharm.* **1992**, *84*, 205–216.
[12] S. Lin-Gibson, V. Srinivasan, *IEEE Trans. Autom. Sci. Eng.* **2019**, *2019*, 1–8.
[13] N. Dragicevic, H. I. Maibach, *Percutaneous Penetration Enhancers Physical Methods in Penetration Enhancement*, Springer, **2017**.
[14] M. E. Lane, *Int. J. Pharm.* **2013**, *447*, 12–21.
[15] M. Sivapragasam, M. Moniruzzaman, M. Goto, *Biotechnol. J.* **2016**, *11*, 1000–1013.
[16] M. Moniruzzaman, Y. Tahara, M. Tamura, N. Kamiya, M. Goto, *Chem. Commun.* **2010**, *46*, 1452.
[17] M. Moniruzzaman, M. Tamura, Y. Tahara, N. Kamiya, M. Goto, *Int. J. Pharm.* **2010**, *400*, 243–250.
[18] M. Zakrewsky, K. S. Lovejoy, T. L. Kern, T. E. Miller, V. Le, A. Nagy, A. M. Goumas, R. S. Lyer, R. E. Del Sesto, A. T. Koppisch, D. T. Fox, S. Mitragotri, *PNAS* **2014**, 111, 13313–13318.
[19] E. L. Eden, K. N. Ibsen, S. Mitragotri, *J. Controlled Release* **2018**, *286*, 137–144.
[20] A. Banerjee, K. Ibsen, Y. Iwao, M. Zakrewsky, S. Mitragotri, *Adv. Healthcare Mater.* 2017, 6, 1601411, 1–11.
[21] X. Wu, Z. Chen, Y. Li, Q. Yu, Y. Lu, Q. Zhu, Y. Li, D. An, J. Qi, W. Wu, *Int. J. Pharm.* **2019**, *558*, 380–387.

[22] A. P. Abbott, D. Boothby, G. Capper, D. L. Davies, R. K. Rasheed, *J. Am. Chem. Soc.* **2004**, *126*, 9142–9147.
[23] F. O. Farias, J. F. Pereira, J. A. Coutinho, L. Igarashi-Mafra, M. R. Mafra, *Fluid Phase Equilib.* **2020**, *503*, 112319–112325.
[24] S. Kaur, A. Gupta, H. K. Kashyap, *J. Phys. Chem. B* **2020**, *124*, 2230–2237.
[25] R. D. Rogers, G. Gurau, *Proc. Natl. Acad. Sci. USA* **2018**, *115*, E10999-E10999.
[26] K. Haerens, E. Matthijs, K. Binnemans, B. Van der Bruggen, *Green Chem.* **2009**, *11*, 1357–1365.
[27] L. Weng, M. Toner Phys, *Chem. Chem. Phys.* **2018**, *20*, 22455–22462.
[28] E. L. Smith, A. P. Abbott, K. S. Ryder, *Chem. Rev.* **2014**, *114*, 11060–11082.
[29] P. Liu, J.-W. Hao, L.-P. Mo, Z.-H. Zhang, *RSC Adv.* **2015**, *5*, 48675–48704.
[30] M. Sakuragi, H. Yoshimura, K. Kusakabe, *Jpn. J. Appl. Phys.* **2020**, *59*, 1–4.
[31] M. Sakuragi, S. Tsutsumi, K. Kusakabe, *Langmuir.* **2018**, *34*, 12635–12641.
[32] Q. Zeng, Y. Wang, Y. Huang, X. Ding, J. Chen, K. Xu, *Analyst.* **2014**, *139*, 2565–2573.
[33] I. M. Aroso, R. Craveiro, Â. Rocha, M. Dionísio, S. Barreiros, R. L. Reis, A. Paiva, A. R. C. Duarte, *Int. J. Pharm.* **2015**, *492*, 73–79.
[34] I. M. Aroso, J. C. Silva, F. Mano, A. S. Ferreira, M. Dionísio, I. Sá-Nogueira, S. Barreiros, R. L. Reis, A. Paiva, A. R. C. Duarte, *Eur. J. Pharm. Biopharm.* **2016**, *98*, 57–66.
[35] Y. Ma, Q. Xia, Y. Liu, W. Chen, S. Liu, Q. Wang, Y. Liu, J. Li, H. Yu, *ACS Omega* **2019**, *4*, 8539–8547.
[36] L. Weng, M. Toner Physical, *Phys. Chem. Chem. Phys.* **2018**, *20*, 22455–22462.
[37] Y. Xie, H. Dong, S. Zhang, X. Lu, X. Ji, *J. Chem. Eng. Data.* **2014**, *59*, 3344–3352.
[38] Y. Dai, J. V. Spronsen, G. J. Witkamp, R. Verpoorte, Y. H. Choi, *Anal. Chim. Acta.* **2013**, *766*, 61–68.
[39] J. A. Bouwstra, A. de Graaff, G. S. Gooris, J. Nijsse, J. W. Wiechers, A. C. van Aelst, *J. Invest. Dermatol.* **2003**, *120*, 750–758.
[40] G. C. Charalambopoulou, T. A. Steriotis, A. C. Mitropoulos, K. L. Stefanopoulos, N. K. Kanellopoulos, A. Ioffe, *J. Invest. Dermatol.* **1998**, *110*, 988–990.
[41] N. Ohta, S. Ban, H. Tanaka, S. Nakata, I. Hatta, *Chem. Phys. Lipids* **2003**, *123*, 1–8.
[42] Y. Obata, I. Hatta, N. Ohta, N. Kunizawa, N. Yagi, K. Takayama, *J. Control. Release.* **2006**, *115*, 275–279.
[43] I. Hatta, H. Nakazawa, Y. Obata, N. Ohta, K. Inoue, N. Yagi, *Chem. Phys. Lipids* **2010**, *163*, 381–389.
[44] R. Esquembre, J. M. Sanz, J. G. Wall, F. del Monte, C. R. Mateo, M. L. Ferrer, *Phys. Chem. Chem. Phys.* **2013**, *15*, 11248–11256.
[45] M. Sakuragi, Y. Takeda, N. Shimada, K. Sakurai, *Polym. Bull.* **2008**, *61*, 107–117.
[46] G. P. Gorbenko, V. M. Ioffe, P. K. Kinnunen, *Biophys. J.* **2007**, *93*, 140–153.

Manuscript received: April 28, 2020
Revised manuscript received: August 7, 2020